A study of uranium-based multilayers: II. Magnetic properties

2008 J. Phys.: Condens. Matter 20 215230

(http://iopscience.iop.org/0953-8984/20/21/215230)

J. Phys.: Condens. Matter **20** (2008) 215230 (9pp) doi:10.1088/0953-8984/20/21/215230

A study of uranium-based multilayers: II. Magnetic properties

R Springell[1,2], S W Zochowski[1], R C C Ward[3], M R Wells[3], S D Brown[2,4], L Bouchenoire[2,4], F Wilhelm[2], S Langridge[5], W G Stirling[2,4] and G H Lander[6]

[1] Department of Physics and Astronomy, University College London, London WC1E 6BT, UK
[2] European Synchrotron Radiation Facility, BP220, F-38043 Grenoble Cedex 09, France
[3] Clarendon Laboratory, University of Oxford, Oxford OX1 3PU, UK
[4] Department of Physics, University of Liverpool, Liverpool L69 7ZE, UK
[5] ISIS, Rutherford Appleton Laboratory, Chilton, Oxfordshire OX11 0QX, UK
[6] European Commission, JRC, Institute for Transuranium Elements, Postfach 2340, Karslruhe, D-76125, Germany

E-mail: ross.springell@esrf.fr

Received 17 December 2007, in final form 25 March 2008
Published 25 April 2008
Online at stacks.iop.org/JPhysCM/20/215230

Abstract

SQUID magnetometry and polarized neutron reflectivity (PNR) measurements have been employed to characterize the magnetic properties of U/Fe, U/Co and U/Gd multilayers. The field dependence of the magnetization was measured at 10 K in magnetic fields up to 70 kOe. A reduction in the magnetic moment was found for all systems. Magnetic 'dead' layers of ∼15 Å were determined for U/Fe and U/Co samples, indicative of chemically diffuse interfaces. For very thick layers, magnetic moments close to the bulk values were expected. For the U/Gd system, a large reduction in the magnetic moment, constant over a wide range of Gd layer thicknesses, was found (∼4 μ_B compared with 7.63 μ_B for the bulk metal). A possible explanation for this behaviour, consistent with observations of the structure of these multilayers, is that the Gd moments are pinned at the boundaries of column-like crystallites within the Gd layers. A study of the effective anisotropy and of a finite-size scaling behaviour of the U/Gd system is also presented. PNR data were collected in a field of 4.4 kOe for U/Fe and U/Co samples (at room temperature) and for U/Gd samples (at 10 K). Model calculations of the reflectivities used inputs extracted from the structural survey carried out on these systems, combined with data from the bulk magnetization measurements.

(Some figures in this article are in colour only in the electronic version)

1. Introduction

The fabrication of artificially layered heterostructures on a nanometre length scale has enabled us to explore the electronic interactions of dissimilar materials in close proximity to one another [1]. Magnetic multilayers represent a class of materials where the surface and interface effects contribute a major component of the properties of the sample as a whole, where the ability to tailor these effects and thus the sample properties, by careful control of the growth conditions, make this a very attractive route to study the properties of condensed matter [2]. This article focuses on the magnetic properties exhibited by multilayers, in particular the combination of a ferromagnetic component with uranium. Uranium is a light-actinide element; it is a paramagnetic metal at room temperature and below with a near temperature-independent susceptibility [3]. It is the first element in the period with an appreciable number of electrons in the 5f band, which has an itinerant character, close to the limit of localization [4]. In fact, ferromagnetism has been predicted at the surface of α-U [5]. We are interested in any interfacial effects that might arise from hybridization of the U 5f electronic band with the electronic states of the ferromagnetic element and investigate the presence of any long-range collective phenomena.

A study of the structural and magnetic properties of the U/Fe system has been reported previously [6, 7]. However,

recent modifications to the fabrication procedure have included the introduction of Nb buffer and capping layers and the use of sapphire substrates, which has improved the multilayer quality. Paper I in this series of articles [8] describes the fabrication and structural characterization of U/Fe, U/Co and U/Gd multilayers in detail. The U/TM (TM = transition metal, Fe, Co) systems showed similar growth characteristics to polycrystalline TM and U layers and a critical thickness for crystallinity of ∼20 Å for the TM layers. The U/Gd system exhibited remarkably good crystalline growth with the Gd present in the bulk *hcp* structure, oriented [00.1]. However the growth of the uranium was unusual and diffraction data suggested the presence of an *hcp*-U phase, oriented [00.1]. The magnetic properties of this phase are unknown and the interaction of its electronic states with those of Gd could reveal some interesting magnetic properties.

This paper will address the bulk magnetic characterization and extend our knowledge of the structure within the U/TM and U/Gd multilayers. A combination of magnetometry and polarized neutron reflectivity (PNR) techniques has been used to investigate the magnetic substructure of the ferromagnetic layers and, for the case of the U/Gd system, to study the anisotropy and magnetic ordering (Curie) temperature as functions of the bilayer composition.

2. Bulk magnetization

2.1. Experimental method

The magnetization measurements were carried out in Quantum Design MPMS (magnetic property measurement system) SQUID magnetometers at UCL and at the Clarendon Laboratory, Oxford. The data were taken using both the DC and the reciprocating sample option (RSO) in no-overshoot mode, which enables a slow stabilization of the field, an important consideration when measuring ferromagnetic signals with a large diamagnetic background, as in our case, due to the relatively thick sapphire substrates. Measurements of the magnetization as a function of applied field were recorded up to 70 kOe, at 10 K, well below the Curie temperatures of iron, cobalt and gadolinium (1043 K, 1388 K and 296 K, respectively).

2.2. U/TM field dependence

Figure 1 presents the saturation magnetization, M_{sat}, plotted as a function of $t_{Fe,Co}$; panel (a) describes the variation of the absolute magnetization, whereas (b) plots the values of magnetic moment per atom. The data in panel (a) were fitted to a linear relationship, which is then presented in panel (b) in units of μ_B/atom. At large values of $t_{Fe,Co}$ (inset of figure 1(b)) M_S tends towards the expected bulk moment values for Fe and Co of 2.2 μ_B and 1.7 μ_B, respectively. The limited number of data points (figure 1(a)) implies some uncertainty in the extremal values of M_S, although it is clear that values close to those of the bulk would be achieved with very thick layers. Values of the saturation magnetization in μ_B/Fe, Co, as determined by polarized neutron reflectivity, are also plotted in figure 1(b); these measurements are described later in the text.

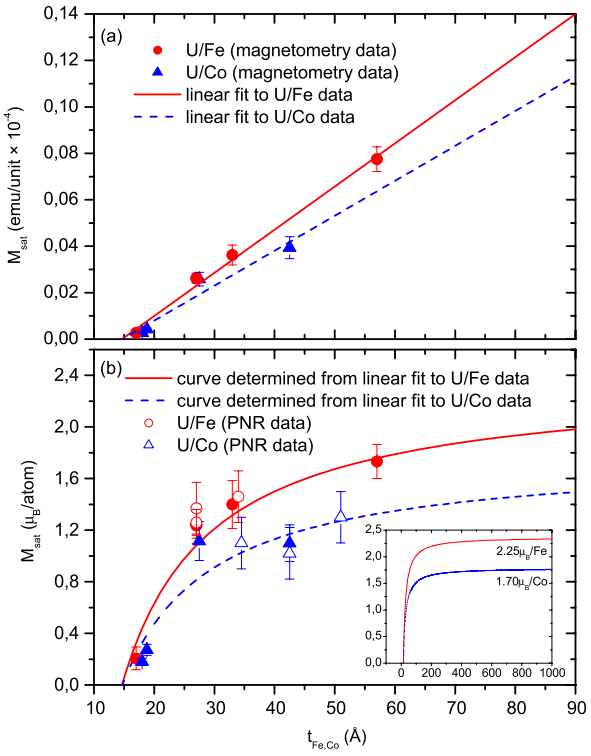

Figure 1. Variation of the saturation magnetization, scaled by the area and number of bilayer repeats, is presented in panel (a), as a function of the ferromagnetic layer thickness with the field applied in the plane of the multilayer. A straight-line fit is shown for both U/Fe and U/Co systems. Values of M_{sat}, given in μ_B/Fe, Co, are shown in (b); the curves are calculated from the fit in (a) and extrapolated to large values of $t_{Fe,Co}$ (inset). Values of M_{sat} as determined by PNR measurements are also presented in (b).

The linear fit to M_{sat} described in figure 1(a) shows a direct proportionality between the increase in Fe or Co layer thickness and the saturation magnetization. The intercept of this line with the x-axis is an indication of the thickness at which there will be no magnetic moment, a magnetic 'dead' layer. However, this distinct separation of a non-ferromagnetic component and a ferromagnetic one is an unrealistic description of the Fe and Co layers. Mössbauer measurements on the U/Fe system [7] can be interpreted in terms of an iron layer comprising three components, $Fe_{amorphous}$, which is paramagnetic, Fe_{bcc} carrying the bulk moment, and a non-magnetic Fe component likely to be present in a U–Fe alloy, where the spin up and spin down 3d bands of the iron can be equally populated; this alloy will be present at both U | Fe and Fe | U interfaces, since one of the principal factors for the formation of these alloy regions is that of chemical interdiffusion, a process independent of the sputtering sequence.

A consideration of the interfacial structure from x-ray diffraction data [8] and results from Mössbauer spectroscopy [7] suggest that the centres of the layers are composed of bulk-like Fe, provided the Fe layers are thicker than the crystalline limit, ∼20 Å [8], and then a U–Fe alloy region will be formed at the interfaces. These interfaces will then include components of non-magnetic Fe, where the concentrations of

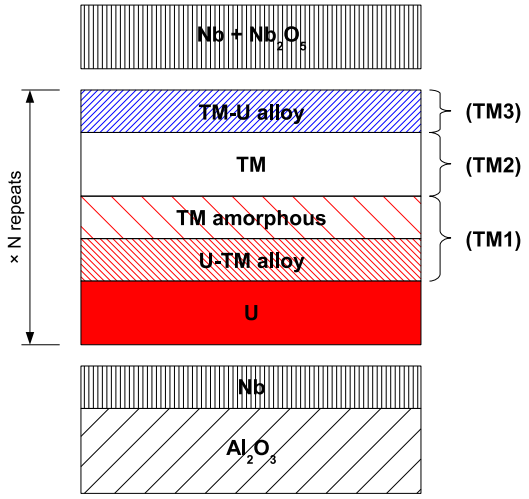

Figure 2. Schematic diagram of an example U/TM multilayer structure, based on the interpretation of Mössbauer [7] and SQUID magnetometry measurements, which has been used to model the distribution of magnetization within a U/TM bilayer.

Fe in U are low, and hence the coordination number of Fe is low. Across the interface from U to Fe, as the concentration of Fe atoms increases, paramagnetic Fe will be found and then ferromagnetic Fe as crystallites of *bcc* Fe form. This result is supported by the x-ray diffraction data presented in paper I [8], which shows that for sample SN72, $[U_{23}/Fe_{17}]_{10}$, there is no visible intensity from any *bcc* Fe component; however, a small magnetic moment is still present. This result suggests that the interface is a complicated mixture of Fe components. The similar atomic size (10.3 $Å^3$ for Co compared with 11.5 $Å^3$ for Fe) and diffusion properties of cobalt are likely to result in a similar interfacial structure and this is supported by the results shown in figure 1.

Although it is not wholly accurate to assign a 'dead' layer thickness, it is a useful tool to compare the extent of the interfaces. In the case of U/Fe and U/Co the values are very similar, 15 ± 2 Å and 16 ± 2 Å, respectively. The formation of such interfaces in transition metal multilayers is not uncommon and has been reported in Ni/Cu [9], Fe/W [10], Fe/V [11], Fe/Nb [12] and Co/Ti [13] systems. A schematic representation of a U/TM bilayer is shown in figure 2. The U/Gd interfaces are sharper than those for U/Fe or U/Co multilayers [8] and do not include such a significant region of interdiffusion. In this case, the magnetic 'dead' layer is expected to be small.

2.3. U/Gd field dependence

A study of the structural properties of uranium multilayers [8], suggests that the U/Gd interfaces are sharper than those for U/Fe or U/Co multilayers and do not include such a significant region of interdiffusion. In the U/TM systems a critical thickness for the onset of crystalline TM layers of $t_{TM} \sim 20$ Å was observed; no such critical thickness was apparent for the U/Gd system. Thus, for the case of U/Gd multilayers the magnetic 'dead' layer is expected to be small.

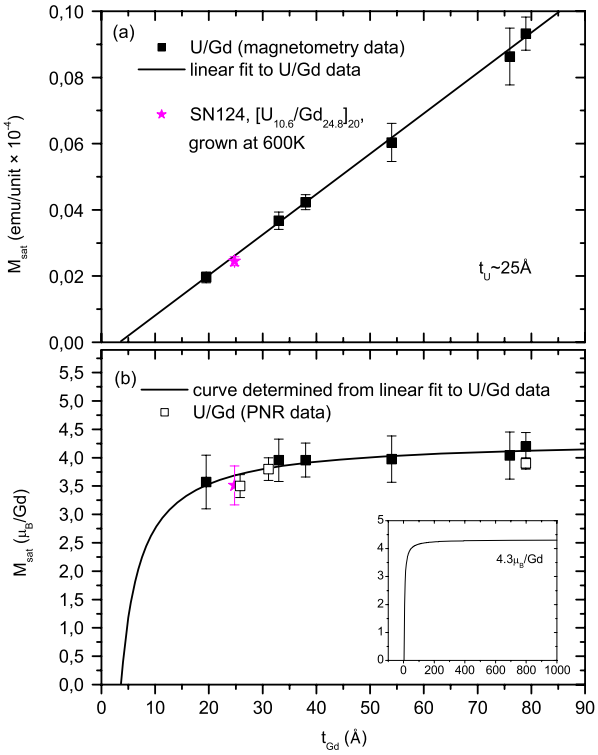

Figure 3. The variation of the saturation magnetization, scaled by the area and number of bilayer repeats, is presented in panel (a) as a function of t_{Gd}. A straight-line fit is shown. Values of M_{sat}, given in μ_B/Gd, are shown in (b) and a curve is presented, calculated from the fit in (a) and extrapolated to large values of t_{Gd} (inset). Values of M_{sat} as determined by PNR measurements (open squares) are also presented in (b).

The saturation magnetization values, M_{sat}, are plotted in figure 3 for samples with $t_U \sim 25$ Å. The field was applied in the plane of the multilayers, H_{para}. A linear relationship is found between the saturation magnetization and the gadolinium layer thickness. The x-axis intercept of the fitted line gives the thickness of the magnetic 'dead' layer, which in this case is 3 ± 1 Å. The inset in panel (b) shows the extrapolated form of the saturation magnetization for large values of t_{Gd}, towards a value of 4.3 μ_B. Figure 3(b) also includes saturation magnetization data obtained from polarized neutron reflectivity data (PNR), described in section 3.

There are some important observations to be made from figure 3. First, the magnetic 'dead' layer of 3 ± 1 Å is significantly thinner than that observed in the U/TM systems. Second, whereas for the U/TM multilayers M_{sat} tended towards the bulk moment value for very thick TM layers (see inset of figure 1(b)) the saturation magnetization extrapolated for large values of t_{Gd} in U/Gd multilayers tends towards a value of 4.3 μ_B, significantly reduced from the bulk metal value of 7.63 μ_B. This indicates that the reduction in magnetic moment is not confined simply to the interface regions, but is an effect arising from the bulk of the Gd layers. Significantly reduced values of the ordered gadolinium moment have been observed in other multilayer systems, such as Gd/Mo [14], Gd/V [15] and Gd/Cr [16]. The possible mechanisms for this phenomenon were discussed for the Gd/Mo system [14] in

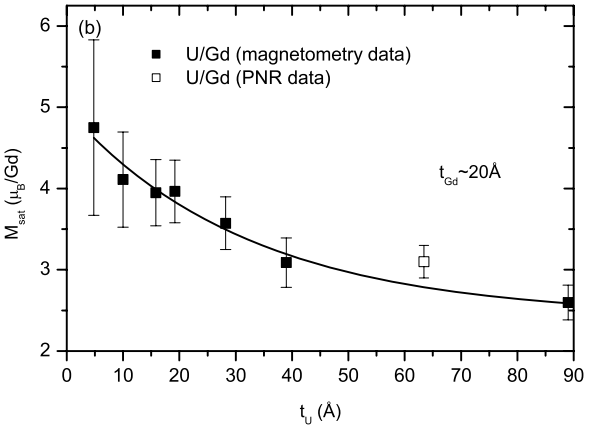

Figure 4. Values of M_{sat} are presented as a function of t_U in units of μ_B/Gd for samples with $t_{Gd} \sim 20$ Å. A PNR measurement is shown as the open square. The solid line is a guide to the eye.

terms of the Gd growth and pinning of the Gd moments at the interface.

The precise mechanism responsible for the low value of the saturated moment is difficult to define. We know that there is a considerable amount of preferred orientation in the Gd layers with the vertical (out-of-plane) direction principally [00.1]. If the layers are thick, for example in a 1000 Å film, then bulk-like behaviour is observed and the easy axis is close to [00.1]. However, we assume that the dipole anisotropy dominates for layer thicknesses <100 Å, as is found for other Gd multilayers [14–16] so that the easy axis is in the plane of the samples (see also section 2.4). For thick Gd layers large roughnesses were observed [8]; these were described as step-like, a feature related to a columnar growth modulation. It is possible that it is at the boundaries of these column structures that the majority of the Gd moments are pinned, although some pinning will also be present at the interfaces.

It is clear, however, that the presence of the uranium layers affects the magnetization of the gadolinium layers. In order to highlight this point, figure 4 shows the saturation magnetization values (μ_B/Gd) for a number of U/Gd samples with a constant gadolinium layer thickness of ∼20 Å. As the U layers become thicker, so the saturation magnetization decays. A likely source of this effect is again a structural one, where variations in t_U can alter the internal strain within the Gd layers, which can in turn affect the pinning of the Gd moments near the U/Gd interface. A similar effect was observed in the Gd/Mo system [17], but in this case a linear relationship was observed between the Mo layer thickness and the reduction in Gd moment. However, the range of Mo layer thicknesses discussed was only between 7 and 15 Å, whereas in our case the U spacer layer thickness varies between 5 and 90 Å.

2.4. Anisotropy

The magnetic anisotropy is a measure of the preferred direction of the magnetization [2], and can be determined directly from bulk magnetization measurements, where the magnetic field is applied both perpendicular to and in the plane of the film. In this investigation a number of U/Gd samples were cut so that the measurements could be made with the samples in both orientations. The resulting hysteresis loops give values for the coercive fields, termed H_C^{para} and H_C^{perp} for the two magnetic field directions, respectively.

The magnetic anisotropy energy, K_{eff} can be determined from the difference in area of the magnetization loops (perpendicular minus parallel); this relationship holds for all directions of the magnetic easy axis. The sign convention adopted for K_{eff} denotes that a positive K_{eff} indicates a perpendicularly oriented magnetic easy axis. The magnetic anisotropy energy or effective anisotropy is primarily a combination of magnetic dipolar (favouring an in-plane alignment) and magnetocrystalline anisotropies, stemming from the long-range magnetic dipolar and spin–orbit interactions, respectively. These contributions can be resolved into volume, K_V, and surface, K_S, contributions to give,

$$K_{eff} = K_V + 2K_S/t_{Gd} \quad (1)$$

K_V is dominated by the magnetic dipolar or shape anisotropy, whereas the lowered symmetry at the interface leads to a dominant spin–orbit effect and therefore surface anisotropy. A plot of the ferromagnetic layer thickness, t, versus tK_{eff} should yield a linear function, where the gradient of the line can be used to calculate the volume anisotropy term and the y-intercept gives twice the surface term.

Although this treatment of the anisotropy of multilayer systems has become commonplace, we note that there are several important assumptions concerning this extraction of the volume and surface contributions from the effective anisotropy. It is assumed that the anisotropy, localized at the interface region, influences the magnetic moments within the bulk of the layer; this is only true if the anisotropy is much smaller than the intralayer exchange, i.e. when the layer is thinner than the exchange length, which is of the order of 50 Å. Also, the validity of the separation of the effective anisotropy into surface and volume terms becomes questionable when the layers are very thin and are almost entirely comprised of interface region.

Table 1 gives H_C^{para}, H_C^{perp} and K_{eff} for selected U/Gd samples. Figure 5(a) shows a plot of $t_{Gd}K_{eff}$ as a function of the gadolinium layer thickness and as a function of the uranium layer thickness. Panel (b) of figure 5 presents the coercive field values as a function of t_U with the applied magnetic field parallel and perpendicular to the plane of the sample.

In bulk *hcp* gadolinium a small uniaxial anisotropy acts to align the spins parallel to the c-axis between the magnetic ordering (Curie) temperature, ∼296 K, and the spin re-orientation transition temperature at ∼230 K [18]. The direction of growth of the gadolinium layers in these U/Gd multilayers is primarily [00.1] [8] so that the uniaxial anisotropy might act to align the moments out of the plane of the film. However, figure 5(a) clearly shows that for all Gd thicknesses investigated, a negative effective anisotropy was measured. This indicates an in-plane alignment of the magnetic moments. A linear fit to the data yields values for K_V and K_S of -1.2 ± 0.3 MJ m^{-3} and 0.28 ± 0.2 mJ m^{-2}, respectively, which are smaller than those obtained for the U/Fe system ($K_V = -1.8$ MJ m^{-3} and $K_S = 2.0$ mJ m^{-2}) [19]. Our

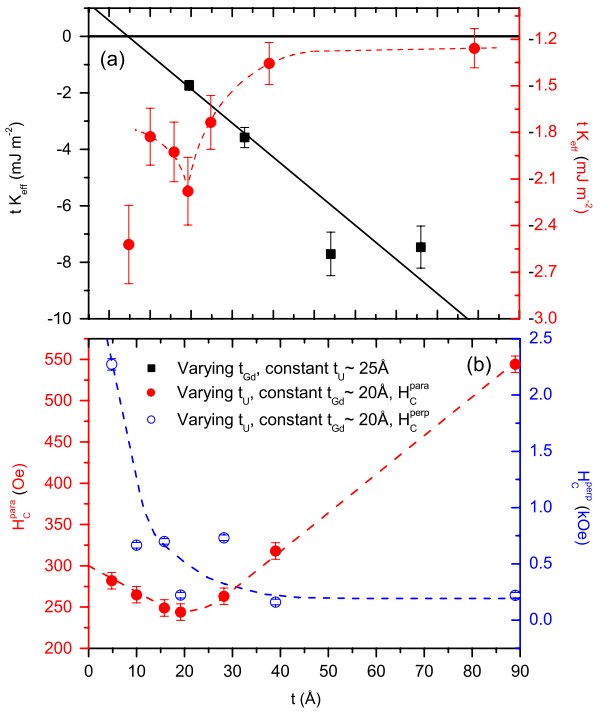

Figure 5. (a) $t_{Gd} K_{eff}$ as a function of t_{Gd} (solid black squares, left-hand axis) and as a function of t_U (solid red circles, right-hand axis). The solid black line is a linear fit to the data. (b) Coercive field values as a function of t_U with the applied magnetic field parallel to the plane of the sample, H_C^{para}, (left-hand y-axis, solid red circles) and perpendicular, H_C^{perp} (right-hand y-axis, open blue circles). Dashed lines are guides to the eye.

values are comparable to those obtained for other Gd thin film systems, such as Gd grown on W, where values of between 0.47 and 1.9 mJ m^{-2} and -1.5 to -0.95 MJ m^{-3} have been reported for K_S and K_V, respectively [20, 21].

The volume term includes contributions from the magnetocrystalline anisotropy, the shape (dipolar) anisotropy and a volume magnetoelastic anisotropy, whereas the surface term is comprised of a surface magnetoelastic effect and a Néel type surface anisotropy, concerned with the symmetry breaking at the interface. The negative slope of the fitted line in figure 5(a), for U/Gd with constant t_U, is a result of the competing shape anisotropy (acting to align the moments within the plane of the film) and surface anisotropy terms (perpendicular alignment). The fitted line extrapolates to a ($t K_{eff} = 0$) thickness of ~5 Å; thus a $[U_{25}/Gd_5]_N$ sample might exhibit perpendicular magnetic anisotropy (PMA). The variation from linearity at large values of t_{Gd} is consistent with the observation of increased interfacial roughness, which is known to affect the anisotropy [22, 23]. The effect of varying t_U on K_{eff} is of a smaller magnitude, however there is a minimum in the anisotropy coincident with the minima of the coercive field data, shown in panel (b).

Figure 5(b) shows the variation in coercive field for different U layer thicknesses for both field directions. A minimum in H_C^{para} can be observed at $t_U \sim 20$ Å. As t_U becomes thinner H_C^{para} changes very little, whereas H_C^{perp} shows a dramatic increase. For thicker U layers the situation is reversed; H_C^{perp} changes very little, but H_C^{para} shows a marked increase. This could be a consequence of the increased strain, a possible explanation for the decrease in M_{sat} seen in figure 4 and consistent with the observation of the anisotropy data in figure 5(a).

Table 1. Summary of the coercive fields, determined from the hysteresis loops, taken with the field applied parallel and perpendicular to the plane of the film. Values of the magnetic anisotropy energy, K_{eff}, calculated as the difference in area of the hysteresis loops, measured in orthogonal field directions are also listed.

Sample	Composition	H_C^{para} (Oe) (±10)	H_C^{perp} (Oe) (±10)	K_{eff} (MJ m^{-3}) (±0.01)
SN63	$[U_{26}/Gd_{33}]_{20}$	350	520	−1.09
SN64	$[U_{26}/Gd_{54}]_{20}$	430	510	−1.43
SN65	$[U_{26}/Gd_{76}]_{20}$	550	810	−0.98
SN66	$[U_{39}/Gd_{20}]_{20}$	320	160	−0.68
SN68	$[U_{89}/Gd_{20}]_{20}$	540	220	−0.63
SN134	$[U_{10}/Gd_{19.8}]_{30}$	270	670	−0.92
SN135	$[U_{15.8}/Gd_{18.2}]_{30}$	250	700	−1.06
SN136	$[U_{19.2}/Gd_{19.4}]_{30}$	240	220	−1.12
SN137	$[U_{28.5}/Gd_{19.5}]_{30}$	260	730	−0.89
SN138	$[U_{4.8}/Gd_{20}]_{30}$	280	2270	−1.26

2.5. *Temperature dependence*

The temperature dependence of the magnetization has been measured for a number of U/Gd multilayer samples with different gadolinium layer thicknesses. Zero field cooled measurements were made between 5 and 375 K in an applied field of 1 kOe with the field applied in the plane of the multilayers. For the purpose of this study T_C was taken as the point at which spontaneous magnetization begins to be observed (i.e. the maximum in the second derivative of the susceptibility).

Figure 6(a) shows the temperature-dependent magnetization curves for a selection of U/Gd multilayers. The variation in lineshapes as a function of the gadolinium layer thickness suggests that the Gd layers consist of regions that have different Curie temperatures, specifically a difference in the behaviour of the centre of the layers and the interface. The dramatic difference between the sample grown at elevated temperature and a sample of similar composition, suggests that it may be strains at the interface region that cause a change in the onset of magnetization, since it is likely that the high temperatures allow the interfacial strain to relax, accommodating dislocations. Panel (b) presents the Curie temperatures for each of these samples as a function of t_{Gd}. The gadolinium layer thickness in this case is given in units of monolayers (1 ML = 2.9 Å [8]). Such a decrease in T_C is well known in thin film systems and can be described by a finite-size scaling relationship [24]:

$$\frac{T_C(\text{bulk}) - T_C(t_{Gd})}{T_C(\text{bulk})} = C_0 \times t_{Gd}^{-\lambda} \qquad (2)$$

where C_0 is an arbitrary constant, which includes contributions from interlayer coupling effects and $\lambda = 1/\nu$, where ν is the

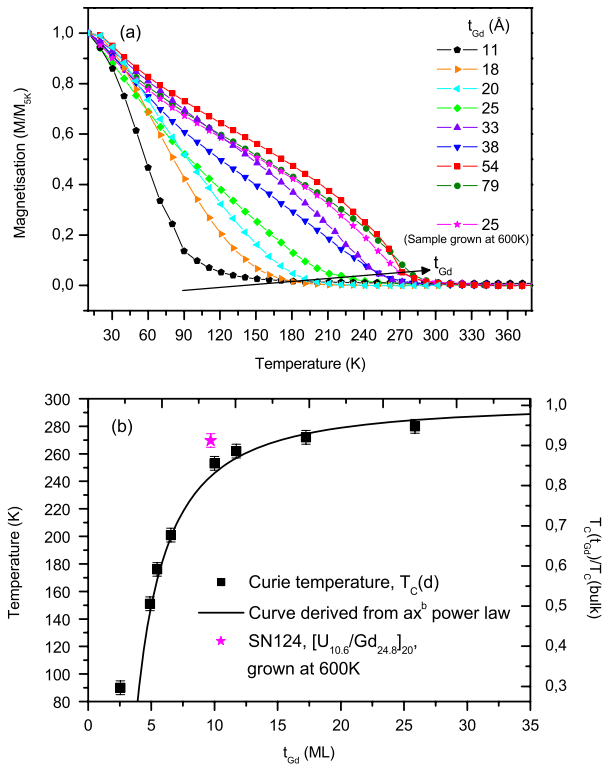

Figure 6. Magnetization as a function of temperature in an applied magnetic field of 1 kOe in the plane of the multilayer is shown in panel (a) for a number of U/Gd samples. The black arrow signifies the direction of increasing Gd layer thickness. Panel (b) plots the Curie temperature as a function of gadolinium layer thickness. The solid black line is a fitted curve to a finite-size scaling relationship, as described in the text.

three-dimensional Ising critical exponent of the correlation length. This treatment of finite-size scaling behaviour describes qualitatively Ni [25], Fe [26], Co [27] and Gd [28] systems studied previously, but includes some assumptions about the nature of the system studied. The size of the magnetic moment is not taken into account and is assumed to have an equivalent value per atom for different layer thicknesses. This requires a coherent multilayer growth with little diffusion at the interfaces. A similar study of the thickness-dependent Curie temperature of gadolinium grown on tungsten [24] reported a finite-size scaling effect and asserted that an observation of this effect in thin films implies a layer-by-layer growth. The solid line in figure 6(b) is the result of fitting to equation (2); this yields values for λ and C_0 of -1.56 and 5.75 respectively. This gives a value for the critical exponent, ν, of 0.64, which is consistent with the 3D Ising model (0.63) [29] and with the relationship observed for the Gd/W thin films [24].

For the U/Gd multilayers with the thinnest gadolinium layers, the observed T_C (90 K) is much higher than that expected from the finite-size scaling behaviour. This has also been observed in the Gd/W system [24] [30] and has been related to the cross-over from 3D to 2D magnetic behaviour, where theory predicts $\nu = 1.00$ in the 2D regime. Sample SN124, grown at a temperature of 600 K, also exhibits a T_C that is higher than that expected. For the Gd/W system [24], higher than expected T_C values were attributed to the accommodation of misfit dislocations and the presence of large inhomogeneous strains, caused by steps and other defects at the interface. The observation of a higher than expected Curie temperature for the U/Gd sample grown at elevated temperature is consistent with these ideas.

3. Polarized neutron reflectivity (PNR)

Neutrons are an extremely useful tool to study simultaneously the chemical and magnetic structure, since they interact with both the nuclei and atomic moments. By aligning a polarized neutron beam normal to the scattering plane and parallel to the sample surface, polarized neutron reflectivity can be used to determine the spin-flip (SF, R^{+-} and R^{-+}) and non-spin-flip (NSF, R^{++} and R^{--}) reflectivities, provided the magnetic field is applied along the quantization direction of the neutron. The difference between the NSF reflectivities is proportional to the magnetization along the field direction, whereas the difference in SF reflectivities is proportional to the square of the magnetization perpendicular to the applied field. Thus, PNR can be used to determine the layer thicknesses and roughnesses, the average magnetic moment per atom, the orientation of the magnetization and the distribution of magnetization in magnetic multilayers.

3.1. Experimental method

PNR measurements were carried out on the CRISP reflectometer of the ISIS time-of-flight neutron source at the Rutherford Appleton Laboratory. U/Fe and U/Co samples were measured at room temperature and PNR data were collected in the specular geometry over a typical Q range of 0.005–0.20 Å^{-1}, in an applied magnetic field of 4.4 kOe, large enough to saturate the magnetization within the plane of the film. U/Gd samples were cooled in zero field to 10 K, well below their Curie temperatures. Only the NSF reflectivity was measured. The xPOLLY programme [31] was used to calculate polarized neutron reflectivities, which were fitted to the experimental data.

3.2. Results

This section presents the experimental data and calculated reflectivities for a selection of U/Fe, U/Co and U/Gd samples. The layer thickness and roughness parameters were fixed at values obtained from x-ray reflectometry. For the case of the U/TM multilayers the large roughnesses accounted for the diffusion at the interfaces, responsible for the magnetic 'dead' layer observed in the bulk magnetization. To analyse the PNR results, the ferromagnetic layers were separated into regions which exhibit a magnetic moment per atom equivalent to the bulk metal, placed at the centres of the layers, and regions with no magnetic moment, at the interfaces. Although it is clear that the layers will not have such discrete sections, it was not possible to distinguish more complex magnetization distributions from the PNR data.

The average magnetization per atom may be accurately determined, by closely monitoring the splitting of the two spin channels at the critical edge, the angle at which the

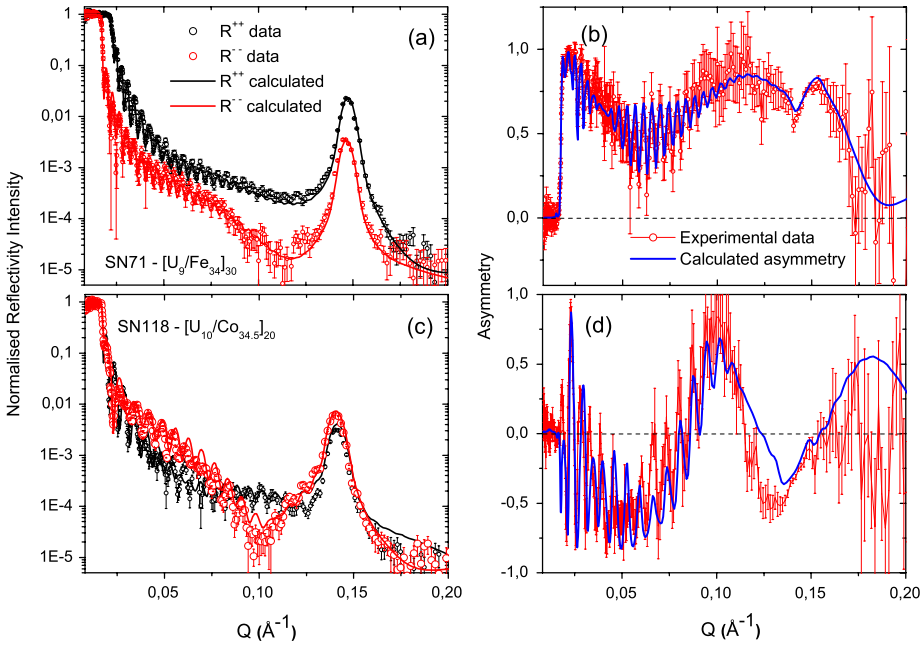

Figure 7. Panels (a) and (c) present the polarized neutron reflectivity data measured in the specular geometry at 300 K and 4.4 kOe for samples SN71, $[U_9/Fe_{34}]_{30}$ and SN118, $[U_{10}/Co_{34.5}]_{20}$, respectively. Experimental data and fitted, calculated curves are shown as black points (curve) for the R^{++} channel and red points (curve) for the R^{--}. The asymmetry for these two samples is shown in panels (b) and (d); red points represent the data and the solid blue line, the fitted calculation.

Table 2. The thicknesses of the three components of the transition metal layers for a selection of U/Fe and U/Co samples, determined from the fitted PNR results.

Sample	Composition	t_{TM1} (±1 Å)	t_{TM2} (±1 Å)	t_{TM3} (±1 Å)
SN71	$[U_9/Fe_{34}]_{30}$	8.0	22.5	3.5
SN74	$[U_{32}/Fe_{27}]_{30}$	8.5	16.2	2.5
SN75	$[U_{35}/Fe_{27}]_{30}$	7.5	15.0	4.5
SN116	$[Co_{42}/U_{19}]_{20}$	11.0	24.0	7.0
SN117	$[U_9/Co_{51.3}]_{15}$	8.0	39.0	4.3
SN118	$[U_9/Co_{34.5}]_{20}$	8.0	22.5	4.0

neutron beam no longer undergoes total external reflection. In this region of the reflectivity curve the splitting of the two spin channels is sensitive to the magnetization of the whole sample. The values for the average magnetic moment per atom determined in this way are shown in figures 1(b), 3(b) and 4.

Figure 7(a) shows the normalized non-spin-flip reflectivity from sample SN71, $[U_9/Fe_{34}]_{30}$. The solid lines represent the calculated reflectivities for both spin channels. Panel (b) displays the asymmetry, determined from the difference divided by the sum of the reflected intensities. Figures 7(c) and (d) present similar results for the U/Co sample, SN118, $[U_{10}/Co_{34.5}]_{20}$.

A model, describing a multicomponent ferromagnetic layer in U/TM multilayers has been proposed in an earlier investigation of U/Fe multilayers [7], but a new interpretation of these components was given in paper I [8] ($UTM_{alloy}|TM_{amorphous}|TM_{bulk}|TMU_{alloy}$) and is shown in figure 2. Table 2 gives the thicknesses for a three-component ferromagnetic transition metal layer. TM1 represents a combination of the UTM_{alloy} and $TM_{amorphous}$ regions and carries no magnetic moment. It has a density that is 5% reduced from that of the bulk material. The central region of the layer, TM2, has equivalent magnetization and density properties to those of the bulk. TM3 includes the TMU_{alloy}. The calculated reflectivities and asymmetries only reproduce the experimental data well when TM1 is greater than TM3, a trend observed for all U/TM samples investigated and consistent with the current description of the growth of U/TM multilayers [8]. The sum of the thickness of layers TM1 and TM3 gives the magnetic 'dead' layer thickness, $\sim 12 \pm 2$ Å, which is close to the value determined by SQUID magnetometry (15 ± 2 Å and 16 ± 2 Å for U/Fe and U/Co, respectively).

Figure 8 shows the experimental data and fitted model for the NSF reflectivity of sample SN63, $[U_{25}/Gd_{33}]_{20}$. The U/Gd samples were modelled by a simple bilayer structure. Figure 2(b) showed that the saturation magnetization did not vary significantly for a wide range of Gd layer thicknesses, indicating a constant distribution of the magnetization within the Gd layers. It is clear from figures 8(a) and (b) that the calculated reflectivities for the NSF channels do not adequately reproduce the data far away from the Bragg peak positions. In particular, the experimental R^{--} intensity is significantly larger in this region than that calculated. This results in a large asymmetry in the calculated case, but very little splitting of the NSF channels in the experimental data. The saturation magnetizations, determined from the splitting of the channels in the vicinity of the critical edge are consistent with SQUID magnetometry measurements. These measurements indicated an even distribution of the magnetic moment through the Gd layers (figure 3(a)). Attempts to introduce a complex

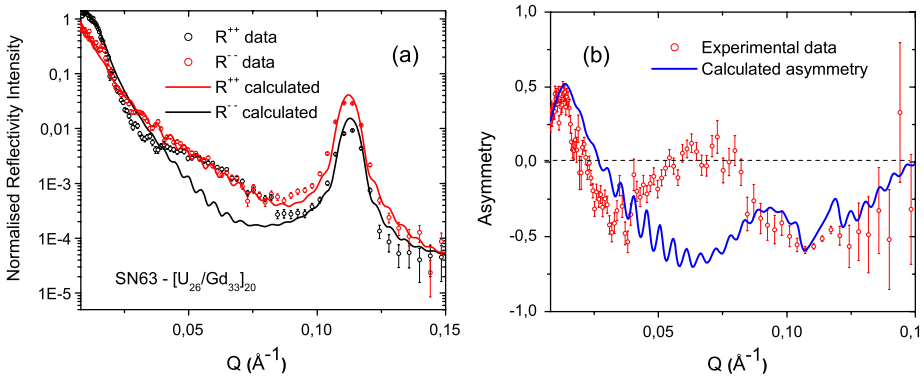

Figure 8. The polarized neutron reflectivity data (panel (a)) and the asymmetry (panel (b)), measured in the specular geometry at 10 K and in an applied magnetic field of 4.4 kOe are presented for sample SN63, $[U_{25}/Gd_{33}]_{20}$. Experimental data and fitted, calculated curves are shown as black points (curve) for the R^{++} channel and red points (curve) for the R^{--}. The asymmetry data are represented by red points and the fitted calculation by the solid blue line.

interfacial structure, as was successful for the U/TM samples, did not result in any improvement in the fit for the U/Gd multilayers.

4. Conclusions

The magnetic properties of U/TM (Fe and Co) and U/Gd multilayers have been determined by a combination of SQUID magnetometry and polarized neutron reflectivity measurements. These results are consistent with ideas developed in paper I [8], concerning the structure and interfacial properties of U/TM and U/Gd systems.

Magnetization measurements on U/Fe multilayers, grown on sapphire substrates with Nb buffer and capping layers, exhibited similar magnetic properties to those grown on glass [7]. This indicates that the predominant effects in this system arise from the interfaces between the two elements. Qualitatively similar effects were reported on the U/Co system. Extrapolated to large values of t_{Fe} and t_{Co}, the saturation magnetization is found to be close to that of the bulk metals. The presence of a magnetic 'dead' layer (∼15 Å) for U/TM multilayers was inferred from both SQUID magnetometry and PNR measurements. However, it was possible to determine a further degree of complexity concerning the TM layers from the PNR data. The experimental data were well modelled by slicing the TM layers into regions with no magnetic moment, on either side of a central bulk-like region. The thicknesses of these slices were consistent with the structural description of the U/TM interfaces developed in paper I [8].

For the U/Gd multilayers, the magnetic moment measured by SQUID magnetometry and PNR was found to be substantially lower than that of bulk gadolinium. However, the mechanism for this reduction is clearly different from that observed in U/TM multilayers. The magnetically 'dead' layer observed for the U/Gd system is 3 ± 1 Å, too small to account for such a large loss in magnetization. This reduction was constant across a wide range of Gd layer thicknesses and cannot be an effect confined to the U/Gd interfaces. A column-like growth, capable of producing the necessary strains and resultant defects in order to pin large numbers of Gd moments is the most likely explanation for this reduction. This picture is consistent with observations of the roughness and crystalline properties described in paper I [8] and with the PNR results.

For U/Gd samples, neither a simple layer structure nor a segmented layer model reproduce the observed experimental data in the PNR experiments. Intensity is observed in the R^{--} channel that is much greater than that expected from model calculations. This effect can be attributed to the large reduction in saturation moment. The pinned moments at the boundaries of column-like gadolinium grains give rise to diffuse scattering, which could contribute to the additional intensity observed. Off-specular measurements will be employed to investigate the diffuse scattering and dichroism measurements will be used to explore any polarization of the U 5f states.

Acknowledgments

RSS acknowledges the receipt of an EPSRC research studentship. We would like to thank Keith Belcher and Peter Clack of the Clarendon Laboratory in Oxford and Tim Charlton and Rob Dalgleish of the CRISP beamline at the ISIS Neutron Source for assistance during sample preparation and neutron experiments, respectively.

References

[1] Camley R E and Stamps R L 1993 *J. Phys.: Condens. Matter* **5** 3727
[2] Bland J A C and Heinrich B 1994 *Ultrathin Magnetic Structures I* (Berlin: Springer)
[3] Bates L F and Hughes D 1954 *Proc. Phys. Soc.* B **67** 28
[4] Freeman A J and Lander G H (ed) 1984 *Handbook on the Physics and Chemistry of the Actinides* vol 1 (Amsterdam: North-Holland)
[5] Stojić N, Davenport J W, Komelj M and Glimm J 2003 *Phys. Rev.* B **68** 094407
[6] Beesley A M, Thomas M F, Herring A D F, Ward R C C, Wells M R, Langridge S, Brown S D, Zochowski S W, Bouchenoire L, Stirling W G and Lander G H 2004 *J. Phys.: Condens. Matter* **16** 8491

[7] Beesley A M, Zochowski S W, Thomas M F, Herring A D F, Langridge S, Brown S D, Ward R C C, Wells M R, Springell R, Stirling W G and Lander G H 2004 *J. Phys.: Condens. Matter* **16** 8507
[8] Springell R, Zochowski S W, Ward R C C, Wells M R, Brown S D, Bouchenoire L, Wilhelm F, Langridge S, Stirling W G and Lander G H 2008 *J. Phys.: Condens. Matter* **20** 215229
[9] Zheng J, Ketterson J B, Falco C M and Schuller I K 1981 *J. Appl. Phys.* **53** 3150
[10] Xiao J Q and Chen C L 1991 *J. Appl. Phys.* **70** 6415
[11] Hosoito N, Kawaguchi K, Shinjo T, Takada T and Endoh Y 1984 *J. Phys. Soc. Japan* **53** 2659
[12] Mattson J E, Sowers C H, Berger A and Bader S D 1992 *Phys. Rev. Lett.* **68** 3252
[13] van Leeuwen R, England C D, Dutcher J R, Falco C M, Bennett W R and Hillebrands B 1990 *J. Appl. Phys.* **67** 4910
[14] Harkins J V and Donovan P E 1996 *J. Phys.: Condens. Matter* **8** 685
[15] Pankowski P, Baczewski L T, Story T, Wawro A, Mergia K and Messoloras S 2004 *Phys. Status Solidi* c **1** 405
[16] Mergia K, Baczewski L T, Messoloras S, Hamada S, Shinjo T, Gamari-Seale H and Hauschild J 2002 *Appl. Phys.* A **74** 1520
[17] Harkins J V and Donovan P 1996 *J. Magn. Magn. Mater.* **156** 224
[18] Kaul S N 2000 *Phys. Rev.* B **62** 1114
[19] Beesley A 2005 Strucural and magnetic studies on sputtered uranium/iron multilayers *PhD Thesis* University of Liverpool
[20] Kalinowski R, Meyer C, Wawro A and Baczewski L T 2000 *Thin Solid Films* **367** 189
[21] Farle M, Platow W, Anisimow A, Schulz B and Baberschke K 1997 *J. Magn. Magn. Mater.* **165** 74
[22] Bruno P 1988 *J. Phys. F: Met. Phys.* **18** 1291
[23] Kim J-H and Shin S-C 1996 *J. Appl. Phys.* **80** 3121
[24] Farle M, Baberschke K and Stetter U 1993 *Phys. Rev.* B **47** 11571
[25] Huang F, Kief M T, Mankey G J and Willis R F 1994 *Phys. Rev.* B **49** 3962
[26] Schneider C M 1990 *Phys. Rev. Lett.* **64** 1059
[27] Qiu Z Q, Pearson J and Bader S D 1993 *Phys. Rev. Lett.* **70** 1006
[28] Jiang J S, Davidovic D, Reich D H and Chien C L 1995 *Phys. Rev. Lett.* **59** 2596
[29] Amazonas M S, Cabral Neto J and Ricardo de Sousa J 2004 *J. Magn. Magn. Mater.* **270** 119
[30] Li Y, Polaczyk C and Riegel D 1998 *Surf. Sci.* **402** 386
[31] Langridge S http://www.rl.ac.uk/largescale/